Left Atrial Structure and Function in Cardiac Amyloidosis

Kotaro Nochioka, MD;[1,2] Candida Cristina Quarta, MD;[3]* Brian Claggett PhD;[1] Gabriela Querejeta Roca, MD;[1] Claudio Rapezzi, MD;[4] Rodney H. Falk, MD;[5] Scott D. Solomon, MD[1]

1 Cardiovascular Division, Brigham and Women's Hospital, Harvard Medical School, Boston, MA, USA

2 Department of Cardiovascular Medicine, Tohoku University Graduate School of Medicine, Clinical Research, Innovation and Education Center, Tohoku University Hospital, Japan

3 Division of Medicine, National Amyloidosis Centre UCL, Royal Free Hospital, London, UK

4 Institute of Cardiology, University of Bologna and S.Orsola-Malpighi Hospital, Bologna, Italy

5 Department of Cardiology, Harvard Vanguard Medical Associates, Brigham and Women's Hospital Cardiac Amyloidosis Program, Harvard Medical School, Boston, MA, USA.

* Co-first author

Address for correspondence:

Scott D. Solomon, MD

Brigham and Women’s Hospital, Cardiovascular Division

75 Francis Street Boston, MA 02115

Phone: +1 857-307-1960 Fax: +1 857-307-1944

Email: ssolomon@rics.bwh.harvard.edu

Abstract

Aims: Although cardiac amyloidosis (CA) is characterized by significant left atrial (LA) dilatation, the characteristics of LA function remain to be fully investigated.

Methods and Results: We assessed LA function by speckle-tracking echocardiography in 124 patients with CA and sinus rhythm: 68 with light chain (AL), 29 with mutant (ATTRm), 27 with wildtype (ATTRwt) transthyretin amyloidosis. Conventional and strain-derived parameters, including LA peak longitudinal strain (LS) and strain rate (peak LSR: reservoir function; early LSR: conduit function; late LSR: active function), were assessed compared between CA patients and 20 healthy controls of similar age and gender.

Results: All LA function phases, including LA longitudinal strain, peak LSR, early and late LSR were significantly impaired in CA compared to healthy controls after adjusting for LA size, LV ejection fraction and LV filling pressures (E/E') (all $p < 0.05$).

Peak LA LS was moderately correlated with LV global LS ($R=-0.60$, $p<0.001$); late LSR was correlated with A wave at the level of LV inflow ($R=-0.69$, $p<0.001$). Among the different CA subtypes, peak LS and LA active emptying fraction were worse in ATTRwt than AL and ATTRm [$p<0.05$ after adjustment for age, sex, body mass index, systolic blood pressure, heart rate, LA volume index, severity of mitral regurgitation, left ejection fraction and left ventricular end-diastolic pressure (E/E')].

Conclusions: In CA, LA function was severely impaired and highly correlated with LV deformation. Differences in LA function between amyloid subtypes suggest that amyloid etiology plays a role in the pathophysiology of cardiac dysfunction in CA.

(250/250)

Keywords: amyloid, cardiomyopathy, left atrial function, echocardiography, 2-dimensional speckle tracking.

Introduction

Cardiac amyloidosis (CA) is caused by intramyocardial amyloid infiltration[1, 2] due to one of several etiologies, including: immunoglobulin light chains (AL) amyloidosis, in which a clonal plasma cell dyscrasia produces the immunoglobulin light chains responsible of the amyloid deposits; hereditary transthyretin (TTR) amyloidosis (ATTRm), which can be caused by over 100 point mutations in the *TTR* gene, and non-hereditary (i.e. wild-type) TTR amyloidosis (ATTRwt), which mainly affects the heart of elderly men.[1, 2]

Amyloid can virtually infiltrate all cardiac chambers. Most studies have focused on the consequences of amyloid infiltration throughout the left ventricle (LV), which include a progressive increase of wall thickness and LV stiffness.[1, 3, 4] Left atrial (LA) or bi-atrial enlargement is a common finding in CA.[5] However, LA enlargement is an anatomical measurement and does not necessarily reflect its function. Although LA size has been reported to be a poor prognostic indicator in CA patients, [6] a comprehensive and quantitative characterization of LA function and its implications in CA is lacking.

Two-dimensional (2D) myocardial deformation imaging is a robust and sensitive echocardiographic technique for the quantitative assessment of LA function [7] and has proven to play an adjunctive role in the diagnosis and prognostic stratification of CA.

We used 2D derived speckle-tracking imaging to characterize LA function in CA and to determine whether the progressive reduction of LA contribution to LV filling is secondary to the restrictive LV physiology, intrinsic LA dysfunction due to direct amyloid infiltration, or a combination of both. We also compared the profiles of the different CA subtypes to investigate whether any observed differences in LA structure and function might account for the reported markedly different prognoses, (median survival ~ 6 months in untreated AL CA vs. 6 years in ATTRwt.[8]

Methods

Setting and study design

We conducted a multicentre retrospective study of patients with etiologically defined CA from two large international amyloidosis centers, the Brigham and Women's Hospital (BWH, Boston) and the S.Orsola-Malpighi Hospital (Bologna). All consecutive patients diagnosed with CA at the Brigham and Women's Hospital (Boston) from 2006 to 2012 (n=110), or at the S.Orsola-Malpighi Hospital (Bologna) from 2009 to 2012 (n=62) as previously reported[4] were reviewed. Patients were included in the present analysis if sinus rhythm was documented at the time of their presentation at either center. We compared their baseline clinical profiles and echocardiographic parameters, with particular focus on LA structure and function, with those of 20 healthy controls retrospectively identified from the medical records of the BWH. Furthermore, we compared the LA indices among the different etiologic subtypes. At the Bologna center, all patients provided informed consent for anonymous publication of scientific data. At the Boston center, the collection of anonymized medical records was approved by the institutional review board.

Definitions of cardiac amyloidosis, etiological subtype and control

Definition of systemic amyloidosis, including etiological diagnosis of AL, ATTRm and ATTRwt amyloidosis, and CA have been previously reported.[4] Briefly, diagnosis of systemic amyloidosis was defined by histological documentation of Congo-red staining and apple-green birefringence under cross-polarized light in at least one involved organ.[9]

Cardiac involvement was defined as an echocardiographic end-diastolic LV wall thickness greater than 1.2 cm (in the absence of any other plausible causes of LV hypertrophy).[1, 2, 10] Other echocardiographic signs suggesting CA (in addition to increased LV wall thickness) included: granular sparkling appearance of the myocardium, increased thickness of atrioventricular valves, right ventricular free wall, or interatrial septum, and pericardial effusion. In selected cases with equivocal echocardiographic findings who did not undergo an endomyocardial biopsy, cardiac

magnetic resonance and nuclear imaging, including ^{99m}Tc-labeled 3,3-diphosphono-1,2-propanodicarboxylic acid (DPD, available in Europe) and ^{99m}Tc-labeled pyrophosphate (PYP, available in the U.S.A.) were performed to confirm the presence and nature of intramyocardial amyloid deposits.[11, 12]

Distinction between AL and TTR-related amyloidosis was based on genotyping and/or immunohistochemistry or mass spectrometry.[1, 9] AL was defined by the presence of monoclonal plasma cell dyscrasia with serum electrophoresis, serum or urine immunofixation, and abnormal serum free light chain assay, in the absence of any TTR mutation at DNA analysis.[13, 14] Diagnosis of familial ATTRm was defined by a documented TTR mutation with DNA analysis following procedures described elsewhere.[15] ATTRwt was defined by positive immunohistochemistry for TTR in the absence of any TTR mutation at DNA analysis.[16] In equivocal cases, biopsy specimens underwent proteomics evaluation.[17]

A group of 20 healthy controls was retrospectively identified from the medical records of the BWH. The search strategy targeted patients aged 55 years or older, who had an echocardiogram, and no International Classification of Diseases 9th Revision (ICD-9) code in their record for any of the following conditions: hypertension, ischemic heart disease, cardiac arrhythmia, dyslipidemia, chronic obstructive lung disease, diabetes mellitus, cerebrovascular disease, arterial vascular disease, and cancer. This group was further selected to have normal LVEF, no LV regional motion abnormalities, normally sized cardiac chambers, no significant valvular disease, and suitable echocardiogram image quality. Controls had a similar age and gender distribution to the CA group.

Echocardiographic Methods

Echocardiograms were performed at both centers using commercially available ultrasound systems (iE33, Philips Medical Systems and Vivid 7, GE Medical Systems, Milwaukee, WI). Images were acquired in DICOM format using a frame rate of 50-70 fps. Analysis of the echocardiographic images (both conventional and speckle tracking-derived measurements) was

conducted at the cardiac imaging core laboratory of the Brigham and Women's Hospital, blinded to clinical information, as previously described.[4] A minimum of 3 cardiac cycles were recorded for each image and measurement were averaged accordingly.

Standard echocardiographic and Doppler parameters were analyzed using an offline analysis workstation. All measurements were made in accordance with the recommendations of the American Society of Echocardiography (ASE).[18-20]

Because dedicated software for LA strain analysis has not yet been released, we used 2D speckle tracking vendor-independent software with algorithms designed for LV analysis (TomTec Imaging Systems, Germany) to study LA deformation.

If more than 2 segments in LA and LV could not be tracked or there was a lack of a full cardiac cycle, missing views, non-DICOM images, significant foreshortening of the cavities, or pulmonary vein drop out for the images focused on the LA, the measurements were considered unreliable and the patient was excluded from the analysis. Speckles were tracked frame by frame throughout the LA and LV myocardium over the course of one cardiac cycle; basal, mid, and apical regions of interest were then created. Semi-quantitative segment tracking was carefully inspected. The LA and LV endocardial borders were traced at the end-diastolic frame. End-diastole was defined by the QRS complex or as the frame after mitral valve closure.

For LV deformation, global longitudinal strain (GLS) was calculated as the average LV longitudinal strain across the 12 segments obtained using apical 4- and 2-chamber views as previously described.[4]

For LA speckle tracking analysis, LA phasic function was measured using volumes and strain indices calculated as the average of the 12 segments obtained using apical 4- and 2-chamber views. LA time-volume curves were generated by calculating LA volume at each phase of the cardiac cycle (LA maximal, LA pre-A, and LA minimum volumes) using the Simpson method. From these LA volumes, LA phasic function was estimated as (**Figure 1A**):

- LA emptying fraction (reservoir function)=([LA maximum volume−LA minimal volume]/LA maximum volume)×100
- LA passive emptying fraction (conduit function)=([LA maximum volume−LA pre-A volume]/LA maximum volume)×100
- LA active emptying fraction (pump function)=([LA pre-A volume−LA minimal volume]/LA pre-A volume]×100

From the LA strain analysis, LA reservoir function was estimated using peak strain during ventricular systole (systolic or peak LA strain), which represents the LA filling during LV systole. Because the LA expands during ventricular systole, peak LA strain is a positive strain value. LA conduit function was estimated using the early peak strain rate (SR) during LV diastole (LA passive strain rate), while LA pump function was estimated using late peak SR during LV diastole (LA active SR). (**Figure 1A** and **1B**).[21-23]

All measurements were performed by a single investigator blinded to clinical status. Intraobserver variability for LA LS and LSR was assessed by measuring three times in the whole sample. The coefficients of variation for LA measures were as follows: LA LS 10.9%, peak LSR 13.2%, early LSR 13.6%, and late LSR 23.5%.

Follow-up

In both centres, follow-up visits were planned for every 6 months (or more frequently if clinically appropriate). Follow-up was closed in 2013, May; for patients who had not attended a visit in the last 6 months, vital status was ascertained by telephone and/or by contacting referring physicians. However, of 124 patients, 11 patients had missing information on death and were excluded from the analysis.

During a median follow-up of 24.4 [17-33] months, we observed 34 (30%) deaths (27 among AL patients, 3 among ATTRm patients, and 4 among ATTRwt patients), with a death rate of

1.8/100 person years among AL patients, 0.3/100 person years among ATTRm patients, and 0.6/100 person years among ATTRwt patients (**Supplementary Figure 1**).

Statistical Analysis

Summary statistics were expressed as mean±SD, median (interquartile range) or numbers (percentages). Comparisons between CA patients and healthy controls were performed using Student's t test for continuous normally distributed variables, Mann–Whitney test for continuous non-normally distributed variables, and Fisher exact test for categorical variables. Pearson's correlation coefficient was used to evaluate the correlation between LA function and age, systolic blood pressure, heart rate, LV function, LV structure, and LA size.

In a subgroup analysis, we divided the CA group into severely enlarged (left atrial volume index (LAVI) ≥48 ml/m^2) and not severely enlarged LA (LAVI<48ml/m^2) according to ASE guidelines.[18, 19]

When comparing the profile of the three different CA subtypes, continuous variables were tested using one-way analysis of variance or Kruskal-Wallis test in case of normally and not normally distributed variables, respectively. Additional comparisons between CA subtypes were performed using multivariable linear regression to adjust for variables that may influence LA size or function, including age, sex, BMI, systolic blood pressure, heart rate, LA volume index to body surface area (BSA), severity of mitral regurgitation, LV ejection fraction and LV end-diastolic pressure as measured by mitral inflow to mitral relaxation velocity ratio (E/E').

Analyses were conducted using STATA 13 SE (Stata Corporation, College Station, TX). All tests were two-sided and a p-value < 0.05 was considered statistically significant.

Results

Study population and baseline characteristics

Of the 172 patients diagnosed with CA during the study period, 124 (72%) were in sinus rhythm at the time of echocardiography and were included in the present analysis (AL, n=68; ATTRm, n=29; ATTRwt, n=27). Among patients with ATTRm, TTR variants were distributed as follows: Ile68Leu (n=8), Glu89Gln (n=6), Val122Ile (n=4), Thr60Ala (n=4), Thr49Ala (n=2), Val30Met (n=1), Arg34Thr (n=1), Glu54Gln (n=1), Gly47Ala (n=1), Thr59Lys (n=1).

Compared to patients in sinus rhythm, those without were older, more frequently male, with a higher prevalence of ATTRm, more advanced heart failure symptoms and more frequent history of heart failure hospitalizations as well as beta blocker and diuretic usage (**Supplementary Table 1**).

Table 1 and **Table 2** summarize the demographic, clinical and echocardiographic findings in the overall CA population (n=124) compared to healthy controls (n=20) and according to the specific etiology of CA, respectively. As expected, all echocardiographic measures, including interventricular septum, posterior wall, LV end-diastolic volume, ejection fraction and GLS, E/E', as well as LA volume and width, were abnormal in CA patients (**Table 1**).

As anticipated, ATTRwt patients were more likely to be elderly males with longer disease duration and a higher degree of both morphological and functional echocardiographic impairment, including thicker cardiac walls and worse contractility and longitudinal systolic function (**Table 2**). No statistical differences were observed among the 3 etiologies of CA in NT-proBNP levels or glomerular filtration rate.

LA structure and function

Table 3 summarizes the LA phasic function in (**A**) CA patients vs. healthy controls and (**B**) according to the specific etiology of CA. Compared to healthy controls, CA patients showed worse strain-derived LA reservoir, conduit and active function, including peak LS, peak LSR, early LSR

and late LSR, even after adjusting for LA volume indexed to body surface area (LAVI), (**Table 3A**).

The unadjusted comparison between AL, ATTRm and ATTRwt (**Table 3B**) did not show any significant differences in LA phasic (reservoir, conduit and active) functions, although ATTRwt showed lower peak LS, peak LSR, early LSR, late LSR and active emptying fraction. LA peak LS was frequently impaired in all etiologies, being abnormal (i.e. under -1.96 SD from the mean value in the control group) in 81%, 74% and 91% of AL, ATTRm and ATTRwt patients, respectively. ATTRwt etiology was associated with significantly lower LA peak LS and LA active emptying fraction when adjusting for age, gender, body mass index, systolic blood pressure, heart rate, LAVI, severity of mitral regurgitation, LV ejection fraction and LV end-diastolic pressure (E/E') (**Table 3B**).

When stratifying CA patients by the severity of LA enlargement (LAVI cut-off=48ml/m^2)[18,19], those with LAVI≥48ml/m^2 showed worse LA reservoir and active function compared to both healthy controls and CA patients with LAVI<48ml/m^2 (**Figure 2**). However, when considering LA conduit function, only LSR was worse in CA patients with severely dilated LA.

Correlation between LA strain measures and other clinical and echocardiographic findings

Overall, in CA patients, LA reservoir, conduit and pump functions were correlated with LV mass index, parameters of LV function and LA size (**Table 4**). LV GLS was correlated with LA peak LS (Pearson R=-0.60, p<0.0001), peak LSR (R=-0.54, p<0.0001) and late LSR (R=-0.54, p<0.0001); a weak correlation between LV GLS and early LSR (R=0.30, p=0.0020) was also observed. Notably, Late LSR also showed a strong negative correlation with A wave measured at the mitral inflow level (R=-0.69, p<0.0001).

Discussion

This is the first study that provides a systematic assessment of LA function in a large cohort of consecutive patients with the three main etiologies of CA.

We showed that all 2D speckle-tracking derived LA phasic functions were severely impaired in CA and highly correlated with LV deformation. LA reservoir function (peak LS) was correlated with LVMI, LV GLS, LV ejection fraction, and diastolic measures and LA dimensions. In our cohort, ATTRwt seemed to show the worst profile of LA function. These findings support speckle-tracking imaging as a sensitive tool to assess LA function in CA and aim to gain further insights into the pathophysiology of LA dysfunction in CA.

Echocardiographically, LA function has been classically studied by means of LA size, phasic volumes, and emptying fraction. In particular, LA dimensions and volumes have been widely correlated with cardiovascular morbidity and mortality in various pathological conditions.[24, 25] However, LA phasic volumes can be influenced by loading conditions. TDI-derived myocardial velocities provide a less load dependant measure of both LV systolic and diastolic function, where a' represents a marker of atrial function. However, TDI measures are angle-dependent and can be influenced by translation and tethering. On the other hand, strain analysis using speckle tracking is a direct measurement of intrinsic LA myocardial deformation, relatively independent of loading conditions and geometric assumptions[26, 27] and with high feasibility and reproducibility.[28]

Previous studies have addressed LA function in CA. Modesto et al showed an impaired reservoir function in AL patients (peak LS and peak LSR) by colour Doppler myocardial imaging. [29] De Gregorio et al showed an impairment in LA reservoir and pump function among patients with TTR-CA and HCM (n=16 in each group), as compared to normal controls, but mainly in the former group, irrespective of LA volume and LV ejection fraction.[30] Our results are consistent with such findings. Indeed, we showed that LA conduit and active functions were impaired in all the three etiologies of CA (**Table 3**). However, when considering LA conduit function, while early LSR was lower in CA than in controls, LA passive emptying fraction did not differ significantly between CA

and controls, suggesting that LA volume changes (conduit function) may be a compensatory mechanism when LA reservoir and pump function are impaired.

Worse LA strain was correlated with a greater impairment of LV systolic and diastolic function. This association suggests that amyloid infiltration progressively impairs both LV and LA function in parallel. A, LV longitudinal systolic dysfunction, which is typical of myocardial amyloid infiltration, may contribute to LA dysfunction because of the influence of downward motion of the mitral plane during ventricular systole, leading to reduced systolic expansion of the LA.[31]

Taken together, our findings support the combination of restrictive LV physiology with raised filling pressures (due to intramyocardial amyloid infiltration) and intrinsic LA failure (due to direct amyloid infiltration) as the main determinant of LA enlargement and dysfunction in CA[21,32] Indeed, in our population LA strain was highly correlated with LV GLS. In addition, a direct injury of LA walls was suggested by the impairment in all LA function phases (independently of LA size), including late LSR (which reflects the intrinsic active LA contraction), that were significantly worse in CA than similar age and gender matched healthy controls, even after adjustment for LA volume, LV systolic and diastolic function. This finding is supported by previous magnetic resonance studies showing a relatively high prevalence of late gadolinium enhancement throughout the LA walls of CA patients.[32] The relatively low prevalence of significant mitral regurgitation in our population suggests that mitral valve disease is not a major factor responsible for LA dysfunction in our patients.[33]

Patients with ATTRwt seemed to show worse LA function parameters compared to the other etiologies of CA, especially AL. It is well known that ATTRwt is a disease characterized by slowly progressive amyloid deposition.[1] Indeed patients with ATTRwt had longer disease duration (median 24.4 months) compared to those with AL (8.6 months) or ATTRm (15.4 months). We therefore anticipated more morphological and functional impairment of both LA and LV in ATTRwt. However, as already reported by our and other groups, the severity of heart failure and survival are

much worse in AL amyloidosis compared to ATTRwt [2, 8] with a median survival of approximately 6 months in untreated AL amyloidosis with heart failure and 6 years in ATTRwt.[2] It was out of the scope of the present study to address the natural history and prognostic role of LA dysfunction among the different etiologies of CA. However, it is likely that in ATTRwt, given the more chronic nature of amyloid deposition, compensatory mechanisms occur to counteract the effects of myocardial amyloid infiltration, including LV hypertrophy. On the contrary, in AL, an acute toxic effect exerted directly on cardiac myocytes[34] or a more rapid rate of amyloid infiltration may lead to LA dysfunction even in the absence of significant LA dilatation. Furthermore, other non-myocardial factors (including multi-organ involvement, autonomic dysfunction, or a direct microvascular infiltration) may play a critical role in the poor prognosis of AL amyloid subtype.[35]

Clinical Implications

Although often ignored, the assessment of left atrial function in CA should be performed routinely in the clinical practice. Indeed, even in the absence of supraventricular arrhythmias such as atrial fibrillation or atrial flutter, patients with CA are predisposed to developing mural thrombi. In one large necropsy series, 26% of patients with cardiac amyloidosis were found to have intra-cardiac thrombi.[36] In another series, 42/156 (27%) CA patients undergoing transesophageal echocardiography were diagnosed with intracardiac thrombi, with a higher frequency in AL vs. other etiologies (35% vs. 18%), despite older age and a higher prevalence of atrial fibrillation in the non-AL group.[37, 38] This phenomenon, which is generally due to atrial standstill derived from markedly increased LV diastolic pressures and intrinsic LA dysfunction, raises concerns regarding the appropriate use of anticoagulation therapy in CA. In this context, the study of LA function by means of standard and speckle tracking deformation imaging could represent a useful clinical tool to identify CA patients with higher thromboembolic risk in whom anticoagulation may be indicated beyond the standard risk scores (including CHADSVASC and CHA_2DS_2VASC).“

Limitations

Several limitations should be noted. This study included a large series of patients with the three main etiologies of CA. However, the absolute number of patients within each etiology is relatively small. To provide reference values of LA strain and strain rate, we selected healthy individuals as controls. However, we acknowledge that the number of age-matched healthy controls was small and we did not compare our findings with those of patients with similar degrees of LA enragement due to other cardiac diseases such as dilated or hypertrophy cardiomyopathy. This may limit our ability to distinguish between the effect of direct amyloid infiltration and more passive effects secondary to LV dysfunction in determining LA dysfunction. The overall advanced stage of the disease presented by CA patients in the present study precludes any possible insights into the earlier stages of CA, which will need a dedicated study. Finally, this study did not include any correlation with clinical outcomes, limiting the power to assess the predictive value of LA strain measurements.

Conclusions

In patients with CA, each phase of LA function assessed by 2D speckle-tracking echocardiography was severely impaired and highly correlated to left ventricular deformation but independent of LA size. The impairment of both passive and active LA function suggests a combination of both LV and intrinsic LA failure in the pathophysiology of LA dysfunction.

Despite the known different clinical courses, LA function was more impaired in ATTRwt compared to AL amyloidosis. This might indicate that in AL, given the more rapid progression of amyloid infiltration and the direct toxic effect exerted by circulating light chains on cardiac myocytes, cardiac dysfunction and heart failure may precede the overt morphological and functional left ventricular and atrial impairment, which seem to be more pronounced in ATTRwt due to a longer course of amyloid deposition.

Funding

This work was partially supported by the grant from the Italian Ministry of Health – GR-2011-02352282 (Dr Quarta).

Disclosures

None

References

1. Falk RH. Diagnosis and management of the cardiac amyloidoses. Circulation 2005;**112**(13):2047-60.

2. Rapezzi C, Merlini G, Quarta CC, Riva L, Longhi S, Leone O, Salvi F, Ciliberti P, Pastorelli F, Biagini E, Coccolo F, Cooke RM, Bacchi-Reggiani L, Sangiorgi D, Ferlini A, Cavo M, Zamagni E, Fonte ML, Palladini G, Salinaro F, Musca F, Obici L, Branzi A, Perlini S. Systemic cardiac amyloidoses: disease profiles and clinical courses of the 3 main types. Circulation 2009;**120**(13):1203-12.

3. Merlini G, Bellotti V. Molecular mechanisms of amyloidosis. N Engl J Med 2003;**349**(6):583-96.

4. Quarta CC, Solomon SD, Uraizee I, Kruger J, Longhi S, Ferlito M, Gagliardi C, Milandri A, Rapezzi C, Falk RH. Left ventricular structure and function in transthyretin-related versus light-chain cardiac amyloidosis. Circulation 2014;**129**(18):1840-9.

5. Falk RH, Quarta CC. Echocardiography in cardiac amyloidosis. Heart Fail Rev 2015;**20**(2):125-31.

6. Mohty D, Pibarot P, Dumesnil JG, Darodes N, Lavergne D, Echahidi N, Virot P, Bordessoule D, Jaccard A. Left atrial size is an independent predictor of overall survival in patients with primary systemic amyloidosis. Arch Cardiovasc Dis 2011;**104**(12):611-8.

7. Kraigher-Krainer E, Shah AM, Gupta DK, Santos A, Claggett B, Pieske B, Zile MR, Voors AA, Lefkowitz MP, Packer M, McMurray JJ, Solomon SD, Investigators P. Impaired systolic function by strain imaging in heart failure with preserved ejection fraction. J Am Coll Cardiol 2014;**63**(5):447-56.

8. Ng B, Connors LH, Davidoff R, Skinner M, Falk RH. Senile systemic amyloidosis presenting with heart failure: a comparison with light chain-associated amyloidosis. Arch Intern Med 2005;**165**(12):1425-9.

9. Benson MD, Breall J, Cummings OW, Liepnieks JJ. Biochemical characterisation of amyloid by endomyocardial biopsy. Amyloid 2009;**16**(1):9-14.

10. Gertz MA, Comenzo R, Falk RH, Fermand JP, Hazenberg BP, Hawkins PN, Merlini G, Moreau P, Ronco P, Sanchorawala V, Sezer O, Solomon A, Grateau G. Definition of organ involvement and treatment response in immunoglobulin light chain amyloidosis (AL): a consensus opinion from the 10th International Symposium on Amyloid and Amyloidosis, Tours, France, 18-22 April 2004. Am J Hematol 2005;**79**(4):319-28.

11. Rapezzi C, Quarta CC, Guidalotti PL, Longhi S, Pettinato C, Leone O, Ferlini A, Salvi F, Gallo P, Gagliardi C, Branzi A. Usefulness and limitations of 99mTc-3,3-diphosphono-1,2-propanodicarboxylic acid scintigraphy in the aetiological diagnosis of amyloidotic cardiomyopathy. Eur J Nucl Med Mol Imaging 2011;**38**(3):470-8.

12. Bokhari S, Castano A, Pozniakoff T, Deslisle S, Latif F, Maurer MS. (99m)Tc-pyrophosphate scintigraphy for differentiating light-chain cardiac amyloidosis from the transthyretin-related familial and senile cardiac amyloidoses. Circ Cardiovasc Imaging 2013;**6**(2):195-201.

13. Lachmann HJ, Booth DR, Booth SE, Bybee A, Gilbertson JA, Gillmore JD, Pepys MB, Hawkins PN. Misdiagnosis of hereditary amyloidosis as AL (primary) amyloidosis. N Engl J Med 2002;**346**(23):1786-91.

14. Palladini G, Perfetti V, Merlini G. Therapy and management of systemic AL (primary) amyloidosis. Swiss Med Wkly 2006;**136**(45-46):715-20.

15. Ferlini A, Fini S, Salvi F, Patrosso MC, Vezzoni P, Forabosco A. Molecular strategies in genetic diagnosis of transthyretin-related hereditary amyloidosis. FASEB J 1992;**6**(10):2864-6.

16. Westermark P, Sletten K, Johansson B, Cornwell GG, 3rd. Fibril in senile systemic amyloidosis is derived from normal transthyretin. Proc Natl Acad Sci U S A 1990;**87**(7):2843-5.

17. Vrana JA, Gamez JD, Madden BJ, Theis JD, Bergen HR, 3rd, Dogan A. Classification of amyloidosis by laser microdissection and mass spectrometry-based proteomic analysis in clinical biopsy specimens. Blood 2009;**114**(24):4957-9.

18. Lang RM, Bierig M, Devereux RB, Flachskampf FA, Foster E, Pellikka PA, Picard MH, Roman MJ, Seward J, Shanewise JS, Solomon SD, Spencer KT, Sutton MS, Stewart WJ, Chamber Quantification Writing G, American Society of Echocardiography's G, Standards C, European Association of E. Recommendations for chamber quantification: a report from the American Society of Echocardiography's Guidelines and Standards Committee and the Chamber Quantification Writing Group, developed in conjunction with the European Association of Echocardiography, a branch of the European Society of Cardiology. J Am Soc Echocardiogr 2005;**18**(12):1440-63.

19. Lang RM, Badano LP, Mor-Avi V, Afilalo J, Armstrong A, Ernande L, Flachskampf FA, Foster E, Goldstein SA, Kuznetsova T, Lancellotti P, Muraru D, Picard MH, Rietzschel ER, Rudski L, Spencer KT, Tsang W, Voigt JU. Recommendations for cardiac chamber quantification by echocardiography in adults: an update from the American Society of Echocardiography and the European Association of Cardiovascular Imaging. J Am Soc Echocardiogr 2015;**28**(1):1-39 e14.

20. Nagueh SF, Appleton CP, Gillebert TC, Marino PN, Oh JK, Smiseth OA, Waggoner AD, Flachskampf FA, Pellikka PA, Evangelista A. Recommendations for the evaluation of left ventricular diastolic function by echocardiography. J Am Soc Echocardiogr 2009;**22**(2):107-33.

21. Rossi A, Gheorghiade M, Triposkiadis F, Solomon SD, Pieske B, Butler J. Left atrium in heart failure with preserved ejection fraction: structure, function, and significance. Circ Heart Fail 2014;**7**(6):1042-9.

22. Cameli M, Lisi M, Mondillo S, Padeletti M, Ballo P, Tsioulpas C, Bernazzali S, Maccherini M. Left atrial longitudinal strain by speckle tracking echocardiography correlates well with left ventricular filling pressures in patients with heart failure. Cardiovasc Ultrasound 2010;**8**:14.

23. Santos AB, Kraigher-Krainer E, Gupta DK, Claggett B, Zile MR, Pieske B, Voors AA, Lefkowitz M, Bransford T, Shi V, Packer M, McMurray JJ, Shah AM, Solomon SD, Investigators P. Impaired left atrial function in heart failure with preserved ejection fraction. Eur J Heart Fail 2014;**16**(10):1096-103.

24. Pritchett AM, Jacobsen SJ, Mahoney DW, Rodeheffer RJ, Bailey KR, Redfield MM. Left atrial volume as an index of left atrial size: a population-based study. J Am Coll Cardiol 2003;**41**(6):1036-43.

25. Moller JE, Hillis GS, Oh JK, Seward JB, Reeder GS, Wright RS, Park SW, Bailey KR, Pellikka PA. Left atrial volume: a powerful predictor of survival after acute myocardial infarction. Circulation 2003;**107**(17):2207-12.

26. Boyd AC, Richards DA, Marwick T, Thomas L. Atrial strain rate is a sensitive measure of alterations in atrial phasic function in healthy ageing. Heart 2011;**97**(18):1513-9.

27. Zhang Q, Yip GW, Yu CM. Approaching regional left atrial function by tissue Doppler velocity and strain imaging. Europace 2008;**10 Suppl 3**:iii62-9.

28. Cameli M, Caputo M, Mondillo S, Ballo P, Palmerini E, Lisi M, Marino E, Galderisi M. Feasibility and reference values of left atrial longitudinal strain imaging by two-dimensional speckle tracking. Cardiovasc Ultrasound 2009;**7**:6.

29. Modesto KM, Dispenzieri A, Cauduro SA, Lacy M, Khandheria BK, Pellikka PA, Belohlavek M, Seward JB, Kyle R, Tajik AJ, Gertz M, Abraham TP. Left atrial myopathy in cardiac amyloidosis: implications of novel echocardiographic techniques. Eur Heart J 2005;**26**(2):173-9.

30. de Gregorio C, Dattilo G, Casale M, Terrizzi A, Donato R, Di Bella G. Left Atrial Morphology, Size and Function in Patients With Transthyretin Cardiac Amyloidosis and Primary Hypertrophic Cardiomyopathy- Comparative Strain Imaging Study. Circulation journal : official journal of the Japanese Circulation Society 2016;**80**(8):1830-7.

31. Timek TA, Miller DC. Experimental and clinical assessment of mitral annular area and dynamics: what are we actually measuring? Ann Thorac Surg 2001;**72**(3):966-74.

32. Kwong RY, Heydari B, Abbasi S, Steel K, Al-Mallah M, Wu H, Falk RH. Characterization of Cardiac Amyloidosis by Atrial Late Gadolinium Enhancement Using Contrast-Enhanced Cardiac Magnetic Resonance Imaging and Correlation With Left Atrial Conduit and Contractile Function. Am J Cardiol 2015;**116**(4):622-9.

33. Cappelli F, Baldasseroni S, Bergesio F, Perlini S, Salinaro F, Padeletti L, Attana P, Paoletti Perini A, Moggi Pignone A, Grifoni E, Fabbri A, Marchionni N, Gensini GF, Perfetto F. Echocardiographic and biohumoral characteristics in patients with AL and TTR amyloidosis at diagnosis. Clin Cardiol 2015;**38**(2):69-75.

34. Brenner DA, Jain M, Pimentel DR, Wang B, Connors LH, Skinner M, Apstein CS, Liao R. Human amyloidogenic light chains directly impair cardiomyocyte function through an increase in cellular oxidant stress. Circ Res 2004;**94**(8):1008-10.

35. Bernardi L, Passino C, Porta C, Anesi E, Palladini G, Merlini G. Widespread cardiovascular autonomic dysfunction in primary amyloidosis: does spontaneous hyperventilation have a compensatory role against postural hypotension? Heart 2002;**88**(6):615-21.

36. Roberts WC, Waller BF. Cardiac amyloidosis causing cardiac dysfunction: analysis of 54 necropsy patients. Am J Cardiol 1983;**52**(1):137-46.

37. Feng D, Edwards WD, Oh JK, Chandrasekaran K, Grogan M, Martinez MW, Syed IS, Hughes DA, Lust JA, Jaffe AS, Gertz MA, Klarich KW. Intracardiac thrombosis and embolism in patients with cardiac amyloidosis. Circulation 2007;**116**(21):2420-6.

38. Feng D, Syed IS, Martinez M, Oh JK, Jaffe AS, Grogan M, Edwards WD, Gertz MA, Klarich KW. Intracardiac thrombosis and anticoagulation therapy in cardiac amyloidosis. Circulation 2009;**119**(18):2490-7.

Figure legends

Figure 1A. Representative examples of left atrial (LA) measurements in a healthy control case. LA maximal volume (Max), LA pre emptying volume (Pre), LA minimal volume (Min), longitudinal strain (LS), and longitudinal strain rate (LSR).

Figure 1B. Representative examples of left atrial (LA) measurements in a patient with advanced cardiac amyloidosis with enlarged LA and lower LA peak LS, peak LSR, early LSR and late LSR.

Figure 2. Comparison of left atrial (LA) function (reservoir, conduit and pump functions) in healthy controls and cardiac amyloidosis (CA) patients with LAvolume index (LAVI)<48 ml/m^2 and CA patients with LAVI>48ml/m^2, bases on *t* test comparison.

Table 1. Demographic, clinical and echocardiographic characteristics in healthy controls vs. cardiac amyloidosis (CA).

	Healthy Controls n=20	CA n=124	P value
Age, yrs	66.5 ± 5.0	64.1 ± 11.9	0.37
Male sex, n (%)	13 (65.0%)	86 (69.4)	0.70
Etiology, n (%)			...
AL	...	68 (54.8)	
ATTRm	...	29 (23.4)	
ATTRwt	...	27 (21.8)	
Systolic blood pressure, mmHg	125 ± 15	119 ± 20	0.27
Diastolic blood pressure, mmHg	72 ± 13	72 ± 10	0.91
Heart rate, bpm	74 ± 19	76 ± 14	0.55
BMI, kg/m^2	24.2 ± 3.8	25.2 ± 4.3	0.33
Echocardiography			
LVEDD, cm	4.4 ± 0.6	4.3 ± 0.6	0.44
IVS, cm	1.0 ± 0.2	1.6 ± 0.3	<0.001
PW, cm	0.9 ± 0.1	1.5 ± 0.2	<0.001
LVEDV/BSA, ml/m^2	53.3 ± 11.8	45.7 ± 11.5	0.017
LVESV/BSA, ml/m^2	22.3 ± 8.2	20.4 ± 7.9	0.38
LV mass index (BSA), g/m^2	81.9 ± 19.0	147.1 ± 42.1	<0.001
LV ejection fraction, %	59.4 ± 3.5	56.0 ± 11.0	0.19
GLS, %	-19.9 ± 2.5	-13.0 ± 4.2	<0.001
E wave, m/s			
A wave, m/s	0.7 ± 0.2	0.6 ± 0.3	0.023
EA ratio	1.0 ± 0.2	1.8 ± 1.0	<0.001
E' (lateral) , cm/s	9.5 ± 2.1	6.1 ± 2.2	<0.001
E/E' (lateral)	7.4 ± 2.0	15.1 ± 7.6	<0.001
A' (lateral), cm/s	10.66 ± 2.63	5.91 ± 2.98	<0.001
S' (lateral), cm/s	8.39 ± 1.71	5.72 ± 2.15	<0.001
LA structure			
LA volume (BSA) ml/ m^2	20.8 ± 4.2	37.7 ± 13.0	<0.001
LA width, cm	3.4 ± 0.4	4.4 ± 0.6	<0.001

Abbreviations: NYHA, New York Heart Association; eGFR, glomerular filtration rate; BMI, body-mass index, LVEDD, left ventricular end-diastolic dimension, IVS, interventricular septum; PW, posterior wall; LVEDV, left ventricular end-diastolic volume, LVESV, left ventricular end-systolic volume, BSA, body surface area; GLS, global longitudinal strain; E/A, early to late mitral inflow velocity ratio; E', lateral mitral early relaxation velocity; A', lateral mitral late relaxation velocity; S', lateral mitral systolic velocity; E/E', mitral inflow to mitral relaxation velocity ratio.

Table 2. Demographic, clinical and echocardiographic characteristics according to the etiological subtype of cardiac amyloidosis.

Total n=124	AL n=68	ATTRm n=29	ATTRwt n=27	P value (AL vs. ATTRm)	P-value (AL vs. ATTRwt)
Age, years	62.1 ± 10.7	59.1 ± 13.1	74.4 ± 6.5*	0.23	<0.001
Male sex, n (%)	43 (63.2)	20 (69.0)	23 (85.2)	0.59	0.036
NYHA class III ot IV, n (%)	15 (22.1)	7 (24.1)	6 (22.2)	0.82	0.99
Systolic blood pressure, mmHg	113.4 ± 17.2	126.0 ± 20.3	126.8 ± 21.5	0.004	0.004
Diastolic blood pressure, mmHg	69.3 ± 9.4	76.0 ± 11.5	73.7 ± 9.9	0.006	0.06
Heartrate, bpm	78.2 ± 13.9	76.1 ± 13.5	70.4 ± 15.6	0.5	0.02
BMI, kg/m	24.8 ± 4.2	26.1 ± 4.4	25.0 ± 4.2	0.17	0.8
Previous history of HF hospitaliation, n (%)	41 (60.3)	11 (37.9)	20 (74.1)*	0.043	0.21
Disease duration,** months	8.6 [3.5, 15.0]	15.4 [5.2, 40.0]	24.4 [6.0, 37.0]	0.021	0.028
Kidney imvolvement†, n (%)	30 (48.4)	0	1 (3.8)	<0.001	<0.001
eGFR, mL/min/1.73m^2	64.6 ± 27.7	73.0 ± 26.9	56.6 ± 17.0*	0.24	0.22
NT-proBNP, median [IQR]	3169 [1321, 12517]	2093 [1111, 3447]	2365 [1255, 4175]	0.1	0.28
Beta blocker, n (%)	18 (27.7)	11 (39.3)	9 (34.6)	0.27	0.51
Ca blocker, n (%)	3 (4.6)	2 (7.1)	0	0.62	0.27
Amiodarone, n (%)	2 (3.0)	1 (3.6)	5 (19.2)	0.89	0.008
Diuretics, n (%)	38 (57.6)	18 (64.3)	21 (80.8)	0.54	0.037
RAS-I, n (%)	12 (18.2)	6 (21.4)	6 (23.1)	0.71	0.59
Echocardiography					
LVEDD, cm	4.2 ± 0.5	4.4 ± 0.6	4.3 ± 0.6	0.018	0.2
IVS, cm	1.5 ± 0.2	1.5 ± 0.3	1.7 ± 0.3*	0.9	<0.001
PW, cm	1.4 ± 0.2	1.4 ± 0.2	1.6 ± 0.2*	0.35	0.002
LV mass/BSA, g/m^2	138.5 ± 36.5	148.0 ± 44.8	167.8 ± 46.1	0.28	0.002
LVEDV/BSA, ml/m^2	44.5 ± 10.7	48.1 ± 11.4	46.1 ± 13.6	0.14	0.55
LVESV/BSA, ml/m^2	19.1 ± 6.6	21.3 ± 9.4	22.7 ± 8.9	0.19	0.033
LV ejection fraction, %	57.5 ± 9.4	56.9 ± 12.6	51.3 ± 11.7	0.79	0.008
GLS, %	-12.6 ± 4.0	-15.2 ± 4.1	-11.7 ± 3.9*	0.006	0.32
E wave, m/s	0.8 ± 0.2	0.8 ± 0.2	0.7 ± 0.2*	0.74	0.036
A wave, m/s	0.6 ± 0.3	0.7 ± 0.3	0.4 ± 0.2*	0.21	0.011
E/A	1.8 ± 0.9	1.6 ± 0.9	2.2 ± 1.1*	0.35	0.07
E' (lateral), cm/s	5.9 ± 2.1	6.8 ± 2.9	5.8 ± 1.2	0.13	0.93
E/E' (lateral)	16.3 ± 8.8	14.0 ± 6.4	12.9 ± 4.5	0.24	0.1
A' (lateral), cm/s	6.1 ± 2.9	6.68 ± 3.40	4.1 ± 1.8*	0.45	0.016
S' (lateral), cm/s	6.0 ± 2.2	5.92 ± 2.34	4.7 ± 1.3*	0.91	0.017
LA volume/BSA, ml/m^2	35.6 ± 12.4	36.7 ± 12.2	44.0 ± 13.9*	0.67	0.006
LA width, cm	4.3 ± 0.5	4.2 ± 0.6	4.8 ± 0.5	0.75	<0.001
Mitral regurgitation, n (%)				0.16	0.16
I	26 (38.8)	6 (21.4)	8 (29.6)		
II	25 (37.3)	9 (32.1)	12 (44.4)		
III	7 (10.4)	1 (3.6)	5 (18.5)		
IV	4 (6.0)	0	0		

Abbreviations: Abbreviations: NYHA, New York Heart Association; eGFR, glomerular filtration rate; BMI, body-mass index, LVEDD, left ventricular end-diastolic dimension, IVS, interventricular septum; PW, posterior wall; LVEDV, left ventricular end-diastolic volume, LVESV, left ventricular end-systolic volume, BSA, body surface area; GLS, global longitudinal strain; E/A, early to late mitral inflow velocity ratio; E', lateral mitral early relaxation velocity; A', lateral mitral late relaxation velocity; S', lateral mitral systolic velocity; E/E', mitral inflow to mitral relaxation velocity ratio.

*Significant (P value<0.05) for AL vs. ATTRwt.

**Disease duration was calculated as the time interval between the onset of symptoms and the final diagnosis of the amyloid disease. The onset of symptoms was derived by patients' self-report of striking changes in their clinical condition in the past weeks/months/years that were judged to be compatible with manifestations of the disease.

†Kidney involvement was defined as the presence of 24-hour urine protein excretion ≥0.5 g/d, and renal insufficiency was defined as glomerular filtration rate <60 mL/min.

Table 3. LA reservoir, conduit and active function

A. Patients with cardiac amyloidosis vs. healthy controls.

LA function	Healthy Controls n=20	CA n=124	Unadjusted P value
Reservoir function			
Peak LS, %	40.6 ± 6.2	18.8 ± 11.6	<0.001*
Peak LSR, S^{-1}	1.60 ± 0.46	0.84 ± 0.47	<0.001*
Total emptying fraction, %	61.0 ± 11.0	45.1 ± 16.7	<0.001*
Conduit function			
Early LSR, S^{-1}	-1.38 ± 0.43	-0.71 ± 0.37	<0.001*
Passive emptying fraction, %	30.7 ± 11.8	25.7 ± 11.3	0.1
Active function			
Late LSR, S^{-1}	-1.48 ± 0.43	-0.84 ± 0.76	0.001*
Active emptying fraction, %	42.3 ± 11.6	28.6 ± 16.6	0.001*

Data are shown as mean ± SD. Abbreviations; LS, longitudinal strain; LSR, longitudinal strain rate.

*Significant (P value <0.05) after adjustment for LA volume index (LAVI), left ventricular ejection fraction and left ventricular end-diastolic pressure (E/E').

B. Within each etiological subgroup

LA function	AL n=68	ATTRm n=29	ATTRwt n=27	Unadjusted P value
Reservoir function				
Peak LS, %	19.3 ± 11.4	20.1 ± 13.9	16.1 ± 9.1†	0.47
Peak LSR, S^{-1}	0.89 ± 0.48	0.88 ± 0.54	0.65 ± 0.29	0.12
Total emptying fraction, %	45.9 ± 17.8	45.7 ± 16.8	42.6 ± 14.0	0.73
Conduit function				
Early LSR, S^{-1}	-0.71 ± 0.34	-0.81 ± 0.53	-0.59 ± 0.21	0.13
Passive emptying fraction, %	25.7 ± 11.7	23.6 ± 11.3	27.8 ± 10.3	0.16
Active function				
Late LSR, S^{-1}	-0.88 ± 0.76	-0.95 ± 0.91	-0.61 ± 0.57	0.28
Active emptying fraction, %	29.5 ± 17.0	31.8 ± 16.9	22.3 ± 14.1*†	0.16

Data are shown as mean ± SD. Abbreviations; LS, longitudinal strain; LSR, longitudinal strain rate.

*Significant (P value<0.05) among groups and †significant (P value<0.05) for ATTRwt vs. AL and ATTRm after adjusting for age, sex, body mass index, systolic blood pressure, heart rate, left atrial volume indexed to body surface area, severity of mitral regurgitation, left ventricular ejection fraction and left ventricular end-diastolic pressure (E/E').

Table 4. Correlation between LA function and age, systolic blood pressure, heart rate, LV function, LV structure, and LA size in patients with CA (n=124)

	Pearson's Correlation (p value)			
	LA reservoir function		LA conduit function	LA pump function
Variables	Peak LS	Peak LSR	Early LSR	Late LSR
Age	-0.25 (p=0.01)	-0.32 (p=0.0012)	0.35 (p=0.0003)	0.12 (p=0.24)
Systolic blood pressure	0.09 (p=0.38)	0.05 (p=0.64)	-0.05 (p=0.67)	-0.14 (p=0.20)
Heart rate	-0.16 (p=0.10)	0.02 (p=0.86)	-0.15 (p=0.12)	-0.04 (p=0.74)
LV structure				
LVEDV/BSA	0.01 (p=0.92)	-0.08 (p=0.42)	-0.07 (p=0.50)	-0.04 (p=0.67)
LV mass index/BSA	-0.28 (p<0.0001)	-0.26 (p=0.0077)	0.08 (p=0.42)	0.22 (p=0.0270)
LV function				
LV GLS	-0.60 (p<0.0001)	-0.54 (p<0.0001)	0.30 (p=0.0020)	0.54 (p<0.0001)
LV ejection fraction	0.48 (p<0.0001)	0.52 (p<0.0001)	-0.27 (p=0.0066)	-0.41 (p<0.0001)
E wave	-0.16 (p=0.11)	-0.06 (p=0.58)	-0.01 (p=0.92)	0.18 (p=0.08)
A wave	0.57 (p<0.0001)	0.55 (p<0.0001)	-0.34 (p=0.0013)	-0.69 (p<0.0001)
E/E' (lateral)	-0.32 (p=0.0030)	-0.25 (p=0.024)	0.20 (p=0.06)	0.26 (p=0.0183)
LA structure				
LA width	-0.36 (p=0.0002)	-0.38 (p=0.0001)	0.41 (p<0.0001)	0.31 (p=0.0017)
LA volume index	-0.36 (p=0.0002)	-0.36 (p=0.0002)	0.30 (p=0.0025)	0.31 (p=0.0021)

Abbreviations: LVEDV, left ventricular end-diastolic volume; BSA, body surface area; GLS, global longitudinal strain; E', lateral mitral early relaxation velocity; A', lateral mitral late relaxation velocity; E/E', mitral inflow to mitral relaxation velocity ratio.

Figure 1A.

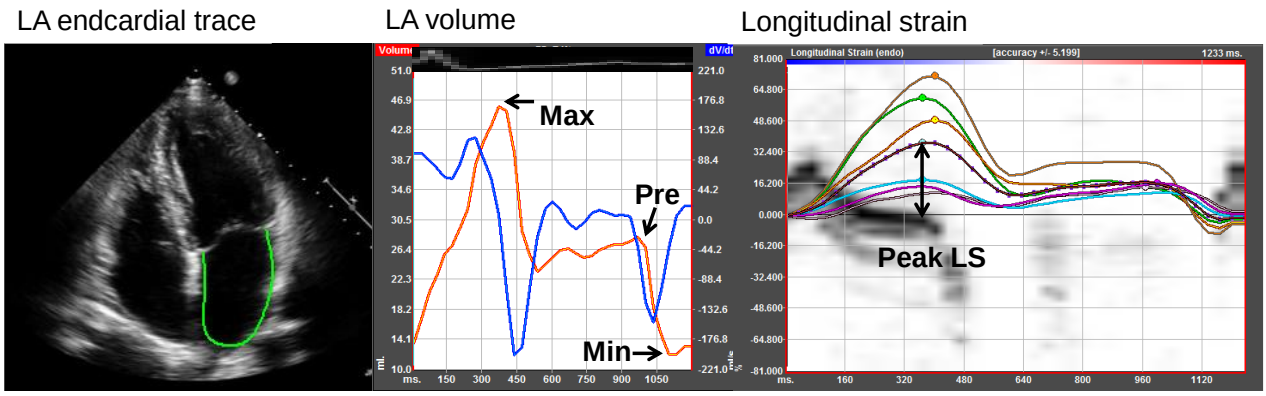

Ventricular phase	Systole	Diastole	
LA function phase	**Reservoir**	**Conduit**	**Active**
Longitudinal strain	Peak LS		
Longitudinal strain rate	Peak LSR	Early LSR	Late LSR
LA volumes: Emptying fraction	Total = Max-Min / Max	Passive = Max-Pre / Max	Active = Pre-Min / Pre

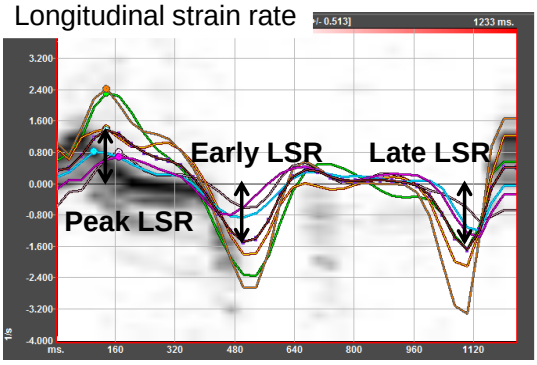

Figure 1B.

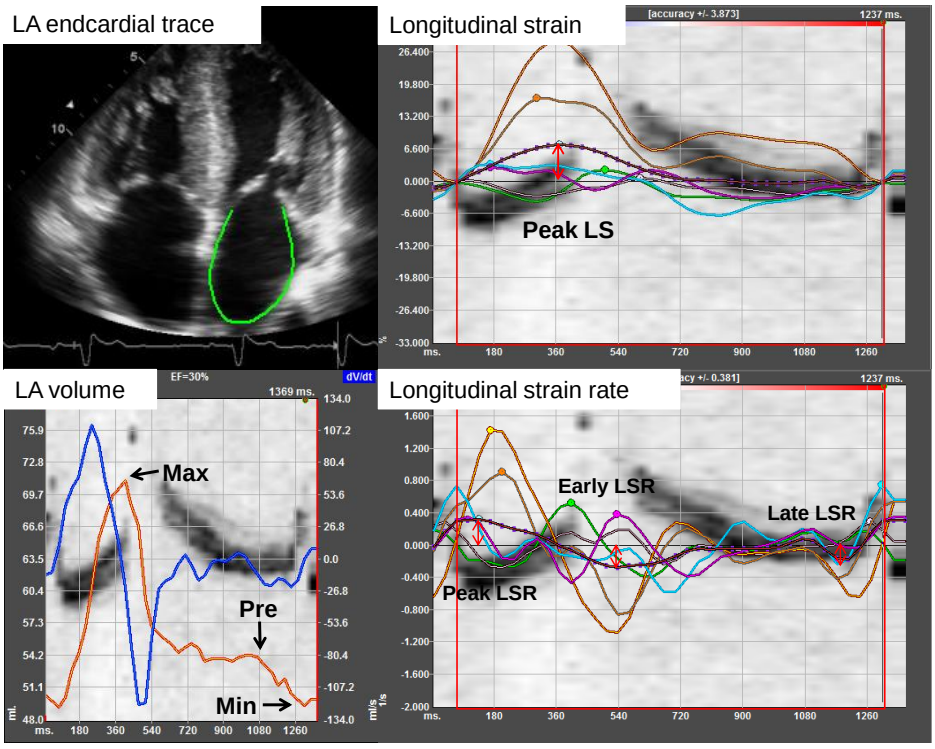

Figure 2.

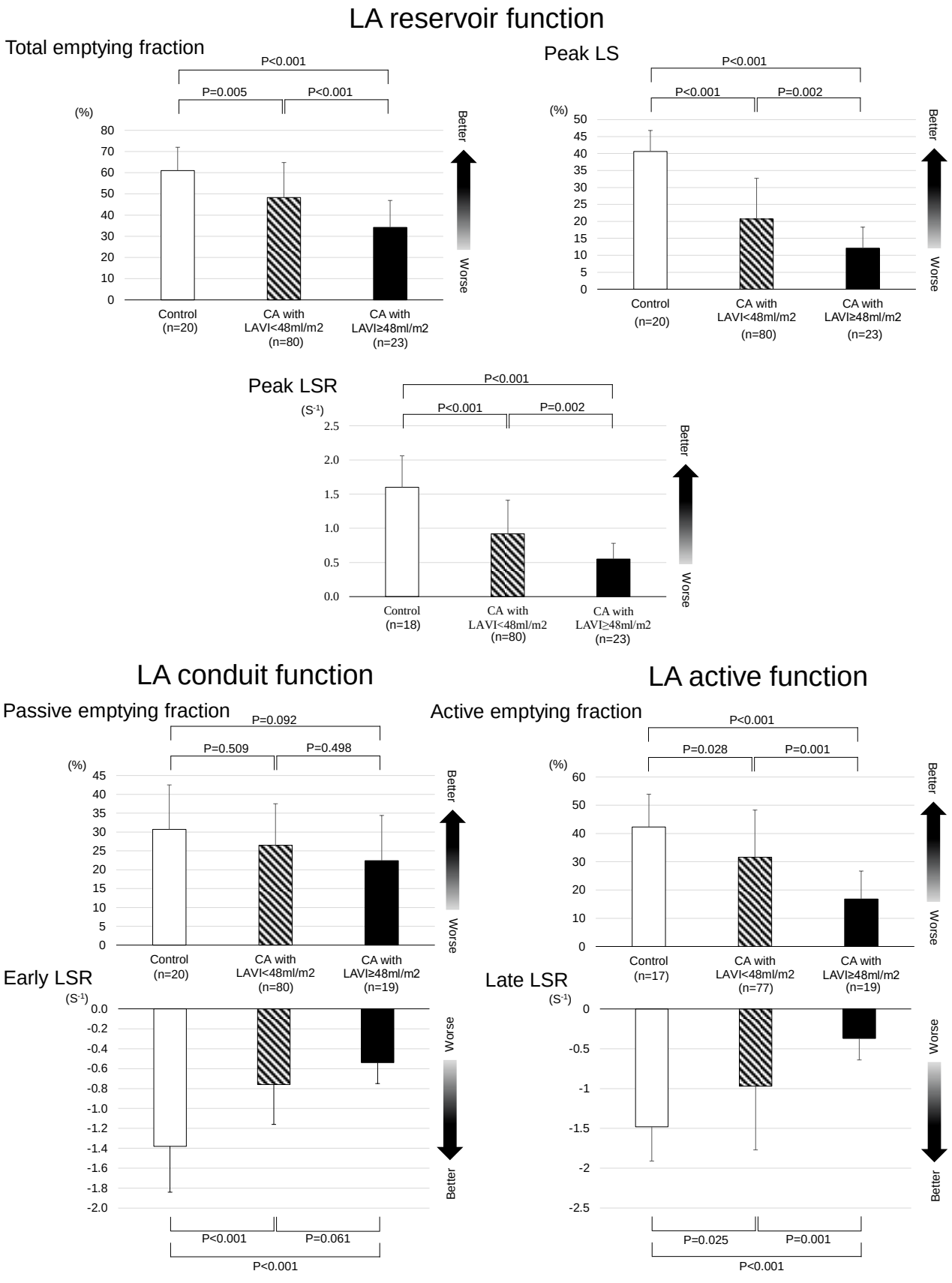
LA reservoir function
Total emptying fraction
P<0.001
P=0.005
P<0.001
(%)
80
70
60
50
40
30
20
10
0
Better
Worse
Control (n=20)
CA with LAVI<48ml/m2 (n=80)
CA with LAVI≥48ml/m2 (n=23)
Peak LS
P<0.001
P<0.001
P=0.002
(%)
50
45
40
35
30
25
20
15
10
5
0
Better
Worse
Control (n=20)
CA with LAVI<48ml/m2 (n=80)
CA with LAVI≥48ml/m2 (n=23)
Peak LSR
P<0.001
P<0.001
P=0.002
(S-1)
2.5
2.0
1.5
1.0
0.5
0.0
Better
Worse
Control (n=18)
CA with LAVI<48ml/m2 (n=80)
CA with LAVI≥48ml/m2 (n=23)
LA conduit function
Passive emptying fraction
P=0.092
P=0.509
P=0.498
(%)
45
40
35
30
25
20
15
10
5
0
Better
Worse
Control (n=20)
CA with LAVI<48ml/m2 (n=80)
CA with LAVI≥48ml/m2 (n=19)
Early LSR
(S-1)
0.0
-0.2
-0.4
-0.6
-0.8
-1.0
-1.2
-1.4
-1.6
-1.8
-2.0
Worse
Better
P<0.001
P=0.061
P<0.001
LA active function
Active emptying fraction
P<0.001
P=0.028
P=0.001
(%)
60
50
40
30
20
10
0
Better
Worse
Control (n=17)
CA with LAVI<48ml/m2 (n=77)
CA with LAVI≥48ml/m2 (n=19)
Late LSR
(S-1)
0
-0.5
-1
-1.5
-2
-2.5
Worse
Better
P=0.025
P=0.001
P<0.001

Supplementary data

Title; Left Atrial Structure and Function in Cardiac Amyloidosis

Authors; Kotaro Nochioka, MD; Candida Cristina Quarta, MD; Brian Claggett PhD; Gabriela Querejeta Roca, MD; Claudio Rapezzi, MD; Rodney H. Falk, MD; Scott D. Solomon, MD

Supplementary Table 1. Comparison of baseline characteristics between included and excluded patients with cardiac amyloidosis

Supplementary Figure 1. Kaplan-Meier Survival Curves for all-cause mortality according to the subtype of cardiac amyloidosis. Curves are turnicated at 60 months.

Supplementary Table 1.

	CA patients without sinus rhythm (Exlcuded) n=44	CA patients with sinus rhythm (Included) n=124	
Age, y	74.1 ± 8.0	64.1 ± 11.9	<0.001
Male sex, n (%)	40 (90.9)	86 (69.4)	0.005
Abnormal rhythm, n (%)			
AF	26 (59.1)	.....	
AFF	2 (4.5)	.....	
AT	2 (4.5)	.....	
PMI	14 (31.8)	.....	
Etiology, n (%)			<0.001
AL	10 (22.7)	68 (54.8)	
ATTRwt	7 (15.9)	29 (23.4)	
ATTRm	27 (61.4)	27 (21.8)	
Disease duration*, median month [IQR]	19.5 [5.0, 33.8]	11.2 [4.2, 28.4]	0.5
NYHA class III to IV, n (%)	23 (52.3)	28 (22.6)	<0.001
Systolic blood pressure, mmHg	115.8 ± 15.6	119.1 ± 19.8	0.34
Diastolic blood pressure, mmHg	69.8 ± 7.8	71.7 ± 10.3	0.29
Heart rate, bpm	75.1 ± 14.9	76.0 ± 14.4	0.73
BMI, kg/m^2	26.5 ± 3.5	25.2 ± 4.3	0.06
History of HF hospitalization, n (%)	39 (88.6)	72 (58.1)	<0.001
eGFR, $mL/min/1.73m^2$	54.8 ± 20.1	64.6 ± 25.9	0.036
Median [IQR]NTPro-BNP, pmol/L	3959 [1289, 6658]	2511 [1307, 4925]	0.7
Medication, n (%)			
Beta blocker	21 (51.2)	38 (31.9)	0.027
Calcium blocker	3 (7.3)	5 (4.2)	0.43
Digitalis	3 (7.3)	2 (1.7)	0.07
Amirodalone	6 (14.6)	8 (6.7)	0.12
Diuretics	39 (95.1)	77 (64.2)	<0.001
RAS-I	13 (31.7)	24 (20.0)	0.12

Abbreviations: AF, atrial fibrillation; AFF, atrial flutter; AT, atrial tachycardia; PMI, pace maker implantation; NYHA, New York Heart Association; eGFR, glomerular filtration rate; BMI, body-mass index; RAS-I, renin angiotensin system inhibitor. *Disease duration was calculated as the time interval between the onset of symptoms and the final diagnosis of the amyloid disease. The onset of symptoms was derived by patients' self-report of striking changes in their clinical condition in the past weeks/months/years that were judged to be compatible with manifestations of the disease.

Supplementary Figure 1.